Volume 1 | Number 1 | Jan 2013 | Pages 1–100

Journal of
Materials Chemistry A

Materials for energy and sustainability
www.rsc.org/materialsA

Li⁺

ROYAL SOCIETY
OF CHEMISTRY

ROYAL SOCIETY
OF CHEMISTRY

www.rsc.org/materialsA

Journal Name

ARTICLE

Rationally Engineered Surface Properties of Carbon Nanofibers on the Enhanced Supercapacitive Performance of Binary Metal Oxide Nanosheets

Ji Hoon Kim[a], Chang Hyo Kim[a], Hyeonseok Yoon[a, b], Je Sung Youm[b], Yong Chae Jung[c], Christopher E. Bunker[d], Yoong Ahm Kim[a,b,*], Kap Seung Yang[a, b,**]

The hybridization of electrochemically active metal oxide with electrically conductive carbon nanofibers (CNFs) has been utilized as a solution to overcome the energy density limitation of carbon-based supercapacitors as well as the poor cyclic stability of metal oxides. Herein, we have demonstrated the growth of binary metal oxide nanosheets on the engineered surface of CNFs in order to fully exploit their electrochemical activity. Metal oxide nanosheets were observed to grow vertically from the surface of CNFs. The high structural toughness of the CNF-metal oxide composite under strong sonication indicated a strong interfacial binding strength between the metal oxide and the CNFs. The rationally designed porous CNFs presented a high specific surface area and showed a high ability of adsorbing metal ions, where the active edge sites acted as anchoring sites for nucleation of metal oxides, thereby leading to the formation of well dispersed and thin layer structure of binary metal oxide nanosheets. An excellent electrochemical performance (e.g., specific capacitance of 2,894.70 F/g and energy density of 403.28 Wh/kg) of these binary metal oxide nanosheets was obtained, which can be explained by the large increase in accessible surface area of electrochemically active metal oxide nanosheets due to their homogeneous distributions on porous CNFs as well as an efficient charge transfer from the metal oxide to the CNFs.

Introduction

Since last decade, supercapacitors have attracted substantial attention as one of the promising energy storage sources for portable devices and electric vehicles because of their higher power density, faster charging time and longer cycle characteristics than those of batteries.[1-3] Especially, carbon-based supercapacitors with high power density and excellent cycle life have been even commercialized.[4,5] However, the main drawback of these supercapacitors is their limited capacitance (or low energy density), which primarily arises from their energy storing mechanism based on physical ion adsorption. On the other hand, pseudocapacitors which utilize fast and reversible Faradic reactions on the surface of metal oxides exhibit high energy density, but at the same time also experience a rapid degradation in their capacitance (or poor cycling life).

To address these issues, hybridization of electrochemically active metal oxide with electrically conducting polymer or carbon materials were examined as a tool to overcome the energy density limitation of carbon-based supercapacitors as well as the instability of metal oxides.[6-11] Among many conducting materials, carbon nanofibers, prepared using electrospinning and followed by a simple carbonization process, were investigated as electrode materials of carbon-based supercapacitors by fully exploiting their intrinsic features, such as nanosized fibrous morphology.[12, 13] Furthermore, the nanosized carbon fibers were also studied as an electrically conductive supporting material of metal oxides to obtain ultrahigh capacity as well as high cyclic performance.[14, 15] More specifically, Zhang and Lou decorated nanostructured $NiCo_2O_4$ on the template-derived carbon nanofibers with a high specific capacitance of 902 F/g[14] while Chen and Zhu showed a high capacitance of 781 F/g by growing $NiCo_2O_4$ on the surface of the carbon fibers.[15]

Although a large volume of research has been devoted in the applications of CNF, discussion on the growth mechanism of binary metal oxides in terms of the surface properties of CNFs is quite limited, even though the nucleation and growth of binary metal oxides are expected to give a profound effect on their morphologies, binding strength and electrochemical performance. To understand the unknown interaction between metal oxide and active sites of carbon materials, and also to achieve a larger capacitive performance of binary metal oxides, we, therefore, carried out a detailed study on the growth of binary metal oxides on two types of surface-modified CNFs. We believe that highly active edge sites on the micropores acted as the nucleation sites for binary metal oxide nanosheets to provide strong binding strength between the metal oxide and CNFs. The rationally designed carbon surface allowed us to achieve an extremely high capacitance up to 2,894.7 F/g because of the large increase in the accessible surface area of electrochemically active metal oxide nanosheets, which are homogeneously and strongly anchored on the surface of porous CNFs as well as a fast charge transfer from electrochemically active metal oxide to electrically conductive CNFs.

Results and discussion
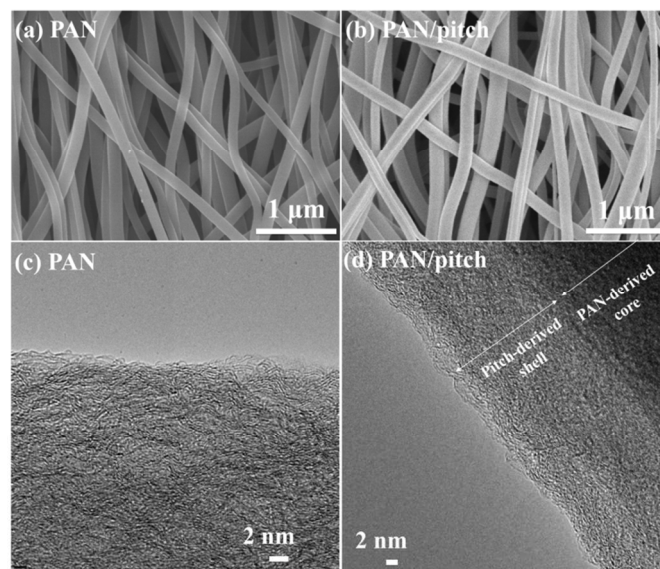
Fig.1 FE-SEM of (a) PAN and (b) PAN/pitch derived carbon nanofibers, and TEM images of (c) PAN and (d) PAN/pitch derived carbon nanofibers.

In order to understand the effect of surface properties of CNFs on the growth of binary metal oxides, we prepared two types of CNFs. One is PAN-based CNFs by electrospinning PAN solution into organic nanofiber in the form of web followed by high temperature thermal treatment. The other is PAN/pitch-based porous CNFs with a high specific surface area from the electrospinning of immiscible PAN and pitch blend into nanofibers followed by high temperature thermal treatment in an inert atmosphere. Both the carbon nanofibers with diameters of ca. 140-150 nm had clean surfaces (Fig. 1 (a, b)). Interestingly, there was no distinctive difference in the fiber morphologies between the two samples based on SEM observation (Fig. 1 (a, b)). However, we observed clear difference in the microtexture between two CNFs through TEM. A typical TEM image of the PAN-derived CNF indicated a disordered structure (Fig. 1 (c)). Long and undulated fringes partially aligned along direction of the length of the CNFs were clearly seen (Fig. 1 (c)). On the other hand, CNFs, prepared from the electrospinning of the immiscible PAN/pitch blend, exhibited a two-phase core-shell structure (Fig. 1 (d)). The shell was composed of low molecular weight pitch, which was possibly due to the solvent evaporation process during electrospinning that pushed the pitch-THF solution toward the outer surface of the nanofibers.[16] Long and randomly curled ribbon-like structures were also observed, possibly due to the different evaporation temperatures of two solvent with regard to PAN and pitch.

Binary metal oxides were then grown on the surface of two different CNFs via a simple chemical process. More specifically, after immersing CNF webs into cobalt and nickel nitrate solution, $NH_3 \cdot H_2O$ was added dropwise to the solution to initiate nucleation of the binary metal oxides on the surface of CNFs. Two different metal ion concentrations (e.g., $Ni(NO_3) \cdot 6H_2O/Co(NO_3)_2 \cdot 6H_2O$ = 2.5/5.0 and 5.0/10.0) were used in the current study, because concentrations lower than 2.5/5.0 led to the growth of indiscernible amount of metal oxide and concentrations higher than 5.0/10.0 induced growth of individually separate

metal oxides without attaching them to the CNFs (see Fig. S1).
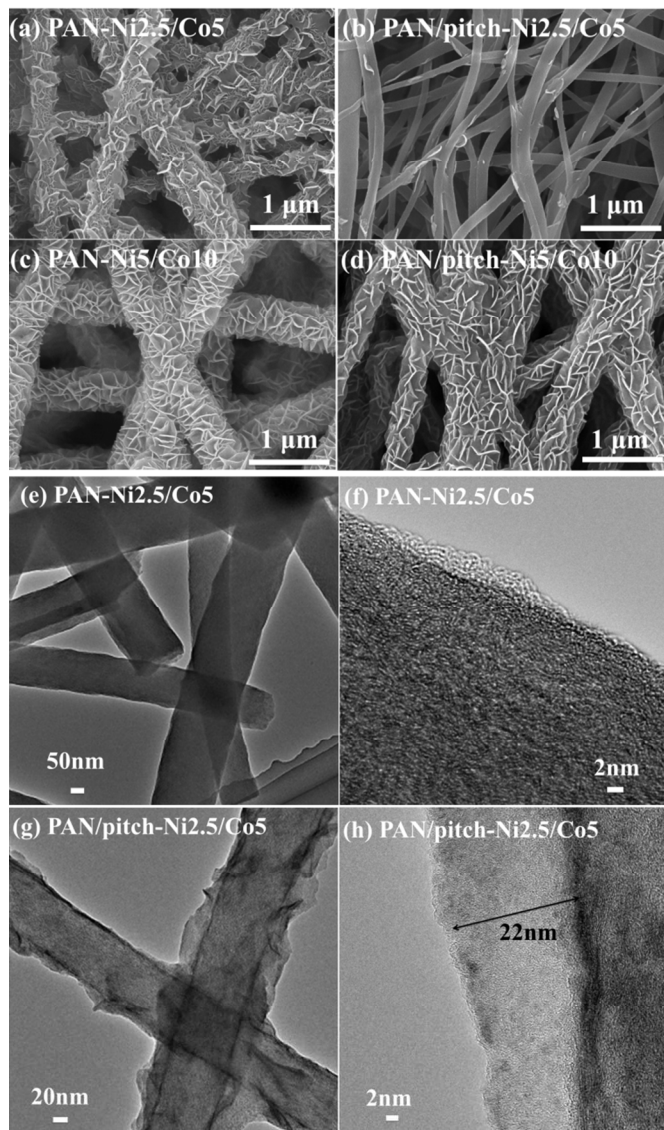
Fig.2 (a-d) FE-SEM, and (d-h) TEM images of binary metal oxide-decorated PAN and PAN/pitched derived carbon nanofibers. (a) PAN-Ni2.5/Co5, (b) PAN/pitch-Ni2.5/Co5, (c) PAN-Ni5/Co10, (d) PAN/pitch-Ni5/Co5, (e) PAN-Ni2.5/Co5, (f) PAN-Ni2.5/Co5, (g) PAN/pitch-Ni2.5/Co5 and (h) PAN/pitch-Ni2.5/Co5.

The growth process allowed CNFs to have beautiful metal oxide nanosheets vertically from the surface of CNFs (Fig. 2 (a-d)). Interestingly, CNFs with high specific surface area, prepared from the electrospinning of PAN/pitch blend solution, exhibited very thin metal oxide sheet around 10 nm (Fig. 2 (d)). Generally speaking, higher the concentration of the metal ion solution, thicker was the binary metal oxide nanosheets on the surface of CNFs. Such results signified strong dependence of morphology and size distribution of binary metal oxide nanosheets on the surface properties of the CNFs. Furthermore, EDX studies revealed that binary metal oxides grown on the surface of the CNFs consisted of carbon, oxygen, cobalt and nickel atoms (Fig. S2). It is interesting to note that the amount of oxygen atoms in the deposited metal oxide showed increased tendency with increasing the amount of metal agent. To see the nanotexture

of the binary metal oxide grown on the surface of CNFs, we carried out detailed TEM observations. Interestingly, a few nm thick binary metal oxide nanosheets were grown on the surface of PAN-derived CNF (Fig. 2 (e, f)), whereas relatively thicker nanosheets (ca. 22 nm) were observed on the surface of PAN/pitch-derived CNF (Fig. 2 (g, h)).
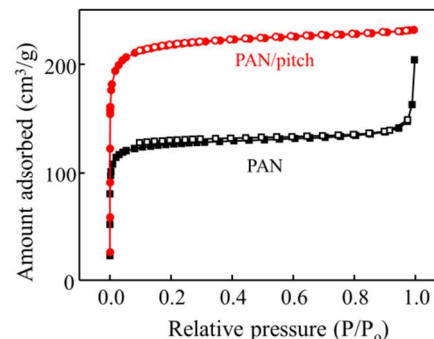
Fig.3 Adsorption isotherms of PAN- and PAN/pitch-derived carbon nanofibers. A large uptake of N_2 below $P/P_0 = 1$ signifies the large amount of micropores smaller than 1.5 nm.

To understand the differently grown metal oxides on PAN- and PAN/pitch-derived CNFs, the surface properties of both carbon nanofibers were further investigated using various analytical tools. As shown in Raman spectra (Fig. S3), there is no distinctive change in the surface crystallinity between the two samples. It is well known that the amount of adsorbed heavy metal ions strongly depends on the amount of functional groups present in the carbon materials.[17] Thus, we also measured FT-IR and XPS to see the differences in the amount of functional groups. However, no significant differences in the oxygen and nitrogen functional groups were found between the two samples (Fig. S4). This can be explained by the fact that we have produced porous CNFs simply by thermally treating immiscible blend without using any commonly used activation process.[16] Furthermore, it is well known that the porosity of activated carbon strongly affects its ability to adsorb heavy metals from aqueous solutions.[18] Therefore to understand the growth pattern of the metal oxides, we compared the pore structure in both the samples through nitrogen adsorption isotherms at 77K. Both the samples followed the type I isotherms without hysteresis.[19] A large uptake of N_2 below $P/P_0 = 1$ in the isotherms of PAN/pitch derived sample signified formation of a large number of micropores smaller than 1.5 nm. As summarized in Table 1, PAN/pitch-derived CNFs showed 1.9 times higher specific surface area, 2.3 times larger total pore volume and smaller average pore diameter as compared with those of PAN-derived CNFs. Thus, we believed that the micropores below 1.5 nm played a predominant role in the growth patterns of binary metal oxides. More specifically, the chemically active edge sites on the wall of pores acted as anchoring sites of metal oxides, resulting in the formation of homogeneously distributed small-sized binary metal oxides on the surface of the microporous CNFs.

Table 1 Pore characteristics of two types of carbon nanofibers.

Sample I.D.	S_{BET} [a] (m^2/g)	V_{micro} [b] (cm^3/g)	V_{total} [c] (cm^3/g)	V_{meso} [d] (cm^3/g)
PAN	494.8	0.181	0.261	0.077
PAN/pitch	856.9	0.337	0.358	0.037

[a] Specific surface area, [b] Micro pore volume, [c] Total pore volume, [d] Mesopore volume.
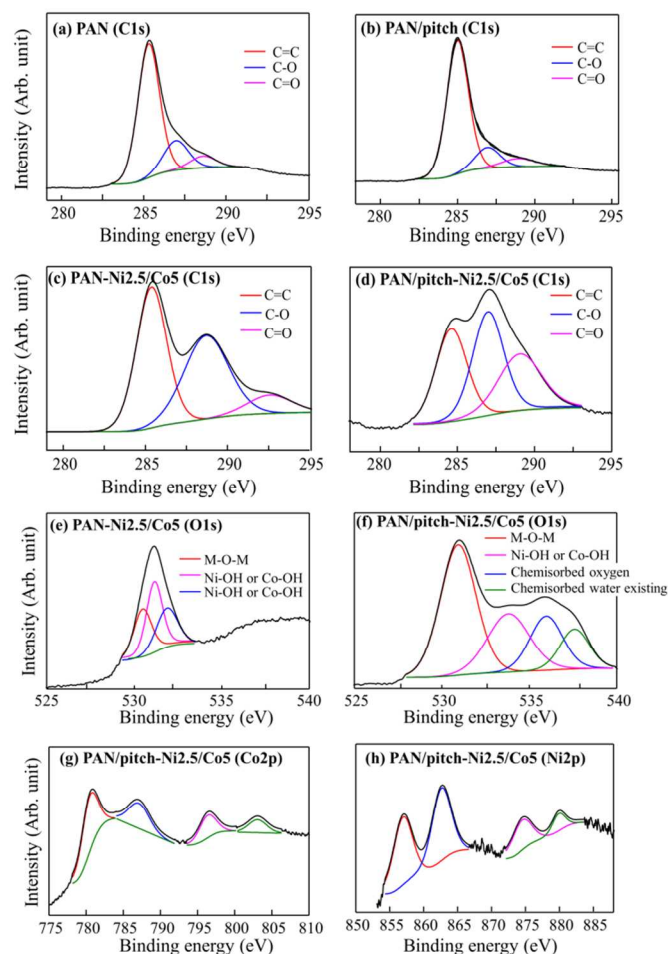
Fig.4 XPS spectra of carbon nanofibers and metal oxide-decorated carbon nanofibers. (a) C 1s of PAN-derived CNFs, (b) C 1s of PAN/pitch-derived CNFs, (c) C1s of PAN-Ni2.5/Co4, (d) C 1s of PAN/pitch-Ni2.5/Co5, (e) O 1s of PAN-Ni2.5/Co5, (f) O 1s of PAN/pitch-Ni2.5/Co5, (g) Co 2p of PAN/pitch-Ni2.5/Co5 and (h) Ni 2p of PAN/pitch-Ni2.5/Co5.

The chemical compositions of the metal oxides on the surface of CNFs were analyzed using XPS. A wide-scan XPS spectrum (Fig. S5) showed that the main components in both the samples were carbon, oxygen, cobalt and nickel. The fine XPS spectra of C 1s, O 1s, Co 2p and Ni 2p displayed more detail information (Fig. 4). In C 1s spectra of PAN and PAN/pitch derived CNFs (Fig. 4 (a, b)), we observed three peaks– the strong peak at 284.6 eV was assigned to sp2-bonded carbon atoms while two broad peaks above 285 eV came from the sp^3-bonded carbon atoms (–C-OH and –COOH)). However, the binary metal deposition on the surface of PAN-derived CNFs caused a large depression of C=C bonded carbon atoms with regard to -COOH (288.1 eV) and -COOR (289.3 eV) (Fig. 4 (c)). A large increase in the intensity of the CO peak suggested a substantial introduction of oxygen atoms during the binary metal oxide deposition process. In case of PAN/pitch-derived CNFs (Fig. 4 (d)), the higher intensity of –C-OH and –COOH in comparison with that of C=C maybe due to the lateral growth of binary metal oxides from the surface of CNFs, at a depth range of 1-10 nm in the XPS. The XPS spectrum for O1s of PAN-Ni2.5/Co5 (Fig. 4 (e)) showed three oxygen species. The peak at 530.5 eV was a typical metal–oxygen bond, the second peak at 531.15 eV corresponded to a large number of defect sites with a low oxygen coordination in the

material with small particle size,[20] and the peak at 531.9 eV can be ascribed to a multiplicity of physically and chemically bonded water both inside and onto the surface. The XPS spectrum for O1s of PAN/pitch-Ni2.5/Co5 (Fig. 4 (f)) showed four oxygen species. The peak at 530.95 eV was metal- oxide peak of M (Ni or Co) corresponding to the C=O groups. The 533.85 eV can be observed Ni-OH and Co-OH groups. The 536 eV peak was chemisorbed oxygen. In addition, PAN/pitch-Ni2.5/Co5 was described binding energy of the chemisorbed water existing (Fig. 4 (f)) at 537.6 eV.[21] In the Co 2p spectrum (Fig. 4 (g)), two kinds of Co species (Co^{2+} and Co^{3+}) were detected. The binding energies at 781.2 and 796.7 eV were ascribed to Co^{3+}. The additional two peaks at 789.5 and 804.9 eV were assigned to Co^{2+}. In the Ni 2p spectrum (Fig. 4 (h)), we also observed two kinds of nickel species containing Ni^{2+} and Ni^{3+}. The peaks at 855.8 and 873.15 eV were assigned to Ni^{2+}, while those at 863.5 and 881.6 eV were assigned to Ni^{3+}.[22]
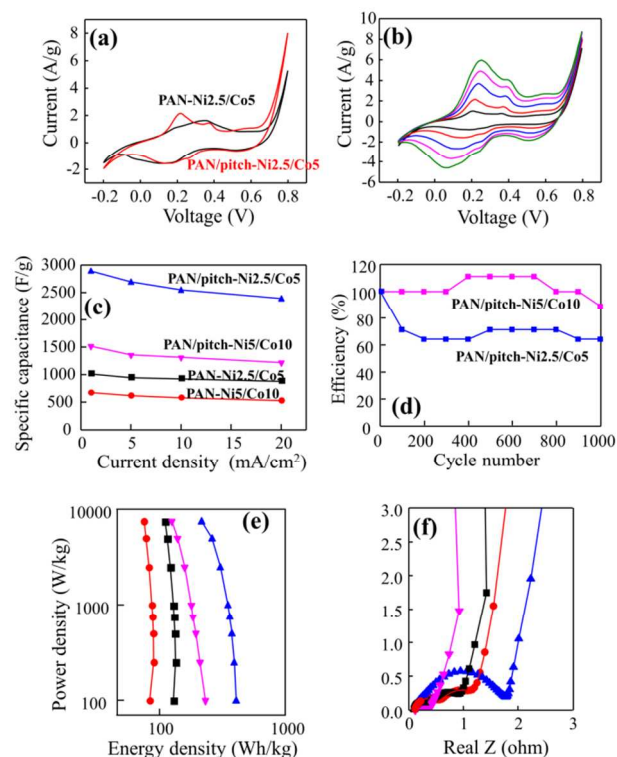
Fig.5 (a) CVs of metal oxides on PAN-Ni2.5/Co5 and PAN/pitch-Ni2.5/Co5 at a scan rate of 25mV/s, (b) The variation of CVs for PAN/pitch-Ni2.5/Co5 in the scan rate from 10 to 100 mV/s, (c) Specific capacitance as a function of current density, (d) The cycling performance of PAN/pitch-Ni2.5/Co5 and PAN/pitch-Ni5.0/Co10 at current density of 1 mA/cm², (e) Ragone plots and (f) Impedance plots at an AC voltage amplitude of 10 mV.

Finally, we carried out electrochemical measurements of the binary metal oxides, which decorated the surface of the CNFs using cyclic voltammetry (CV), and electrochemical impedance (EIS). Figure 5 (a) shows CV of the binary metal oxides on PAN- and PAN/pitch derived CNFs using a scan rate of 25mV/s. The CV of both samples consisted of a well-defined pair of strong redox peaks within the potential range from -0.2 to 0.8V. Binary metal oxides on PAN-derived CNFs showed an oxidation and a reduction peak at 0.35 and 0.12 V, respectively. On the other hand, the metal oxides on PAN/pitch-derived CNFs revealed two oxidation peaks around 0.22, 0.37 and a reduction peak around 0.15V. Such

a slight shift in the peaks can be explained by the full utilization of metal oxides with regard to electrolyte ions, especially at low scan rate. Figure 5 (b) shows the CVs of PAN/pitch-Ni2.5/Co5 in 6M KOH electrolyte at different scan rates in the range 10–100 mV/s. The CVs were almost symmetric, indicating good reversibility of the oxidation and reduction processes. The CVs showed a broad redox peak due to faradic reactions of cobalt hydroxide and nickel hydroxide.[23, 24] In Fig 5 (c) the specific capacitance is plotted as a function of the discharge current density ranging from 1 to 20 m A/cm^2, based on the gram of binary metal oxides. Since CNF webs obtained from the electrospinning of PAN and PAN/pitch blends exhibited high electrical conductivity and relatively good mechanical strength,[16, 25] they can be used as current collector in the fabrication of flexible and thin supercapacitors. Noticeably, the highest specific capacitance achieved was around 2,800 F/g. Note that the specific capacitances of both PAN and PAN/pitch nanofibers without decorating binary metal oxides are 87.9 and 130.7 F/g, respectively. Zhang and Lou showed an extremely high specific capacitance of 902 F/g using the judicious coating of nanostructured NiCo$_2$O$_4$ on carbon nanofibers,[14] whereas Chen and Zhu showed a high capacitance of 781 F/g by decorating NiCo2O4 on the electrospun PAN-derived carbon nanofibers.[15] In comparison, our sample exhibited an extremely high capacitance of 2,800 F/g due to the following reasons. First, when preparing the electrode for the electrochemical measurement, our studies did not use conductive filler and polymeric binder because of the intrinsic free-standing nature of the electrospun-derived carbon nanofiber sheet. In contrast, two previous studies prepared the electrode consisting of the active material, carbon black and polymeric binder.[14, 15] Secondly, a high specific surface area (ca. 856 m^2/g) in the PAN/pitch-derived carbon nanofiber signifies the higher amount of active sites (such as chemically active edges) on the surface of carbon nanofibers which eventually acted as anchoring sites for the homogeneous growth of binary metal oxides. In other words, the extremely high accessible surface area of binary metal oxides with regard to the electrolyte as well as good electron transfer from binary metal oxide to carbon nanofiber contribute to the higher specific capacitance than previously reported studies. The binary metal oxides on PAN/pitch derived CNFs exhibited two times higher capacitance than those on the PAN derived CNFs. Moreover, the decreased capacitance when increasing the amount of bimetal reagents is the limited number of active sites due to the over-grown binary metal oxides. In order to examine the cyclic stability of binary metal oxides, we carried out the repeated charging and discharging process up to 1,000 cycles for PAN/pitch-Ni2.5/Co5 and PAN/pitch-Ni5/Co10 sample (Fig. 5 (d)). In case of PAN/pitch-Ni2.5/Ni5.0, we observed the continuous loss of the specific capacitance up to 200 cycles, but there is no degradation in the specific capacitance up to 1000 cycles. However, PAN/pitch-Ni5.0/Co10 exhibited the excellent cyclic performance up to 1,000 cycles. Based on the Ragone plot (Fig. 5 (e)), we achieved high energy density in the range of 83.7 – 403.3 Wh/Kg at a power density of 100–10,000 W/ kg. In addition, the ac impedance measurements were carried out to evaluate the electrical resistance in the frequency range of 100 KHz-100 MHz (Fig. 5 (f)). Small arcs indicated that the charge transfer resistance between the electrode and the electrolyte was small, because the size of

the electrolyte ion was believed to be well-matched with the pore size of CNFs. The steep linear slopes at low frequencies indicated that the adsorption of ions onto the electrode surface were rapid and followed the kinetics of ion diffusion in solution. The internal solution resistance (R_s) and the charge transfer resistance (R_{ct}) were obtained as 0.1 Ω and 0.3-1.7 Ω, respectively for various samples. Furthermore, we observed an increase in R_{ct} with increasing metal concentration for the PAN-derived CNFs. By contrast, an opposite tendency was obtained for the PAN/pitch-derived CNFs. Thus, it can be assumed that binary metal oxide nanosheets on PAN/pitch-derived CNFs may be more suitable for high power applications.

Conclusions

In summary, to fully exploit the pseudo-capacitive performance of metal oxides with a good cyclic property, binary metal oxides were decorated on the surface of the electrospun PAN and PAN/pitch-derived CNF webs via a simple chemical method. Beautiful nanosheets were coated or vertically grown on the surface of these CNFs. We observed that the pore structure of CNFs (e.g., specific surface area and pore size) largely affected the morphologies of the coated metal oxide nanosheets. More specifically, it is believed that the chemically active edge sites in predominantly present micropores acted as nucleation sites to grow metal oxide nanosheets heterogeneously, resulting in the formation of homogeneously distributed small sized binary metal oxides. As a result, the full utilization of metal oxides with regard to the electrolyte ions and rapid electron transfer between the metal oxides and the carbon surface could be the main reasons for achieving the largest specific capacitance (2894.7 F/g) as well as the maximum energy density (403.3 Wh/kg)

Experimental

Synthesis of Two Types of Carbon Nanofibers

Polyacrylonitrile (PAN, 3.33g, Pfaltz & Bauer Chemical CO. USA) was dissolved in dimethylformamide (DMF, 30g, Duksan Chemical Co., Korea) whereas isotropic pitch (1.42g, Hanwha Chemical Co., Korea) was dissolved in tetrahydrofuran (THF, 5.71g). Isotropic pitch (30%) and PAN (10%) solutions were blended. Finally, both solutions (PAN and PAN/pitch) were electrospun using a voltage of 25 kV and a tip-to-collector distance of 18 cm. The electrospun organic nanofiber web was air-stabilized at 280°C for PAN and 300°C for PAN/pitch. Finally, both fiber webs were carbonized at 1000°C in a horizontal furnace under nitrogen flow at a heating rate of 5°C/min

Growth Procedure of Ni-Co Binary Oxide Nanosheets

The reagents (Co(NO$_3$)$_2$·6H$_2$O, Ni(NO$_3$)$_2$·6H$_2$O and NH$_3$·H$_2$O) (Aldrich Chemical Co., USA) were used to grow binary metal oxides on the surface of CNFs. Various molar ratios of Ni(NO$_3$)·6H$_2$O/ Co(NO$_3$)$_2$·6H$_2$O at 2.5/5.0 (0.72g/1.45g) and 5.0/10.0 (1.44g/2.9g) were dissolved in 35 ml of deionized water. PAN-, PAN/pitch-derived CNF webs were immersed in cobalt and nickel nitrate solution and then NH$_3$·H$_2$O (3ml) was added dropwise over 15 minutes in air with stirring. The chemically grown Ni-Co metal oxides on CNFs were then washed several times with

deionized water and ethanol, followed by drying in a vacuum oven at 120°C for 14hrs. The weight percent of the deposited metal oxides on the surface of PAN/pitch-Ni2.5/Co5.0, PAN/pitch-Ni5.0/Co10.0, PAN-Ni2.5/Co5.0 and PAN-Co5.0/Ni10.0 were calculated to be 4.26, 8.00, 10.00 and 12.14 %, respectively.

Structural Characterizations

The morphological and textural changes of CNFs before and after the growth of binary metal oxide were characterized using a field-emission scanning electron microscope (FE-SEM, Hitachi, S-4700, Japan) and a High-resolution transmission electron microscopy (HRTEM, JEM2100F, JEOL, Japan). The chemical state of the surface of the CNFs before and after the growth of binary metal oxides was examined by X-ray photoelectron spectroscopy (XPS, MULTILAB 2000 SYSTEM) spectrometer. Specific surface areas were analysed by the BET method using an ASPS 2020 Physisorption Analyzer (Micromeritics, USA).

Electrochemical Analysis

Electrochemical behaviors of the three-electrode system and two electrode cells for supercapacitors were evaluated, viz. cyclic voltammetry (CV), charge and discharge (CD), power and energy density (PD) and impedance. CV measurements were done using a three-electrode system using modified Glassy carbon electrode (GC) as the working electrode, a Pt plate as the counter electrode, and Ag/AgCl(saturated KCl) as the reference electrode using for Rotating disk electrode. The binary metal oxide nanosheets coated porous CNF web with diameter of 5mm was cut to a disk-shape, and directly adhered to the surface of GC by 5μL of Nafion solution (0.5 wt. %).[26] CV was obtained in the potential range of -0.2-0.8 V at a scan rate of 10-100 mV/s in a 6M KOH aqueous solution.

To measure CD, PD and impedance, a cell was used containing 2.25 cm^2 electrodes with nickel current collector on the surface of the electrode. Samples used for the electrode were prepared without using a polymer binder. The electrode performance was evaluated in 6M aqueous KOH at room temperature. The capacitance of the electrodes was galvanostatically measured with a WBCS3000 battery cycler system (WonATech Co., Korea) in the potential range of 0.0-1.0 V and at a current density of 1-20 mA/cm^2. The cell capacitance was calculated from the slope of the discharge based on Eq. (1);

$$C = i\,(\Delta t/\Delta V) \text{ ----- (1)}$$

where C is the capacitance of the cell in farads (F), i is the discharge current in amperes (A), Δt is the discharging time from 0.6 to 0.5 V (approximately 60–50% of the initial voltage), ΔV is the voltage variation in the time range measured, and the slope is in volts per second (V/s).

In a symmetrical system, the specific capacitance Cm in farads per gram of sample (F/g) is related to the specific capacitance of the cell, C, as shown in Eq. (2);

$$C_m = 2C/m \text{ ----------- (2)}$$

where m is the weight (g) per metal oxides.

The energy density was measured as a function of constant power discharge in the range of 100-7,500 W/kg. The ac impedance measurements were performed in the frequency range of 100 kHz to 100 MHz using an electrochemical impedance analyzer (Jahner Electrik IM6, Germany).

Notes and references

a Department of Polymer Engineering, Graduate School, Chonnam National University, 77 Yongbong-ro, Buk-gu, Gwangju 500-757, Republic of Korea
Fax: +82-62-530-1774; Tel: +82-62-530-1774; E-mail: ksyang@jnu.ac.kr
b Alan G. MacDiarmid Energy Research Institute and School of Polymer Science and Engineering, Chonnam National University, 77 Yongbong-ro, Buk-gu, Gwangju 500-757, Republic of Korea.
Fax: +82-62-530-1779; Tel: +82-62-530-1871; E-mail: yak@jnu.ac.kr
c Institute of Advanced Composite Materials, Korea Institute of Science and Technology (KIST), Chudon-ro 92, Bongdong-eup, Wanju-gun, Jeonbuk 565-905, Republic of Korea.
d Air Force Research Laboratory, Aerospace Systems Directorate, Wright-Patterson Air Force Base, Ohio 45433-7103, USA.

† Electronic Supplementary Information (ESI) available: [SEM image, EDX, Raman and XPS result]. See DOI: 10.1039/b000000x/

1   P. Simon, Y. Gogotsi, *Nat. Mater.* 2008, **7**, 845-854.
2   P. Simon, Y. Gogotsi, B. Dunn, *Science* 2014, **343**, 1210-1211.
3   G. P. Wang, L. Zhang, J. J. Zhang, *Chem. Soc. Rev.* 2012, **41**, 797-828.
4   L. L. Zhang, X. S. Zhao, *Chem. Soc. Rev.* 2009, **38**, 2520-2531.
5   T. Chen, L. Dai, *Materials Today* 2013, **16**, 272-280.
6   Z. Fan, J. Yan, T. Wei, L. Zhi, G. Ning, T. Li, F. Wei, *Adv. Funct. Mater.* 2011, **21**, 2366-2375.
7   H. Wang, C. M. B. Holt, X. Tan, B. S. Amirkhiz, Z. Xu, B. C. Olsen, T. Stephenson, D. Mitlin, *Nano Res.* 2012, **5**, 605-617.
8   L. Y. Chen, Y. Hou, J. L. Kang, A. Hirata, T. Fujita, M. Chen, *Adv. Energy Mater.* 2013, **3**, 851-856.
9   J. Xu, Q. Wang, X. Wang, Q. Xiang, B. Liang, D. Chen, G. Shen, *ACS Nano* 2013, **7**, 5453-5462.
10 C. Y. Foo, A. Sumboja, D. J. H. Tan, J. Wang, P. S. Lee, *Adv. Energy Mater.* 2014, **4**, 1400236.
11 J. Ji, L. L. Zhang, H. Ji, Y. Li, X. Zhao, X. Bai, X. Fan, F. Zhang, R. S. Ruoff, *ACS Nano* 2013, **7**, 6237-6243.
12 C. Kim, B. Thi Nhu Ngoc, K. S. Yang, M. Kojima, Y. A. Kim, Y. J. Kim, M. Endo, *Adv. Mater.* 2007, **19**, 2341-2436.
13 M. Inagaki, Y. Yang, F. Kang, *Adv. Mater.* 2012, **24**, 2547-2566.
14 G. Zhang, X. W. Lou, *Scientific Reports* 2013, **3**, 1470.
15 L. Chen, J. Zhu, *Chem. Commun.* 2014, **50**, 8253-8256.
16 B.-H. Kim, K. S. Yang, Y. A. Kim, B. An, K. Oshida, *J. Power*

Sources 2011, **196**, 10496-10501.

17 A. Stafiej, K. Pyrzynska, *Sep. Purif. Technol.* 2007, **58**, 49-52.

18 K. Pyrzy?ska, M. Bystrzejewski, *Colloids Surf A* 2010, **362**, 102-109.

19 J. T. Nolan, T. W. McKeehan, R. P. Danner, *J. Chem. Eng. Data* 1981, **26**, 112-115.

20 J.-C. Dupin, D. Gonbeau, P. Vinatier, A. Levasseur, *Phys. Chem. Chem. Phys.* 2000, **2**, 1319-1324.

21 Y. Ge, K. Kan, Y. Yang, L. Zhou, L. Jing, P. Shen, L. Li, K. Shi, *J. Mater. Chem.* A 2014, **2**, 4961-4969.

22 J.-G. Kim, D. L. Pugmire, D. Battaglia, M. Langell, *Appl. Surface Sci.* 2000, **165**, 70-84.

23 V. Gupta, S. Gupta, N. Miura, *J. Power Sources* 2008, **175**, 680-685.

24 L. Huang, D. Chen, Y. Ding, S. Feng, Z. Lin Wang, M. Liu, *Nano Lett.* 2013, **13**, 3135-3139.

25 E. Zussman, X. Chen, W. Ding, L. Calabri, D. A. Dikin, J. P. Quintana, R. S. Ruoff, *Carbon* 2005, **43**, 2175-2185.

26 Q. Guo, D. Zhao, S. Liu, S. Chen, M. Hanif, H. Hou, *Electrochimica Acta* 2014, **138**, 318-324.

The table of contents entry

Ji Hoon Kim, Chang Hyo Kim, Hyeonseok Yoon, Je Sung Youm, Yong Chae Jung, Christopher E. Bunker, Yoong Ahm Kim,* Kap Seung Yang**

Title: Rationally Engineered Surface Properties of Carbon Nanofibers on the Enhanced Supercapacitive Performance of Binary Metal Oxide Nanosheets
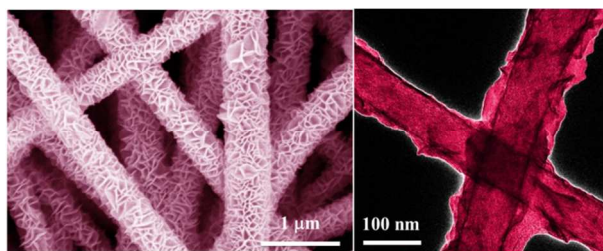
The electrochemically active binary metal oxide nanosheets on the surface of the electrically conductive and porous carbon nanofibers exhibited high pseudo-capacitive performance.